Supplementary Materials

Electrochemical Dealloying High-chromium Alloy Under Oxygen Evolution Potential

Lijia Ning[1], Chunmei Yang[1*], Guannan Jiang[2], Chenglin Wang[3], Shuaishuai Wang[2], Yang Chen[1], Huanxi Zheng[2*], Xin Liu[2], Jiyu Liu[1*]

[1] *College of Mechanical and Electrical Engineering, Northeast Forestry University, Harbin 150000, China.*

[2] *State Key Laboratory of High-Performance Precision Manufacturing, Dalian University of Technology, Dalian 116024, China.*

[3] *Key Laboratory for Light-weight Materials, Nanjing Tech University, Nanjing 211816, China.*

[*]*Corresponding authors: Prof. Chunmei Yang (ycmnefu@126.com), Prof. Huanxi Zheng (huanxizh@dlut.edu.cn), Prof. Jiyu Liu (liujiyu19940802@163.com)*

LSCM images of polarized high-chromium alloy surfaces

Laser scanning confocal microscope (LSCM) images were observed to further investigate the current oscillation behavior. The ultra-chromium alloy samples were polarized under 6 $V_{Ag/AgCl}$ and micro-morphologies were observed every 20 s, as shown in Fig. S1. At the beginning of the polarization process, high surface porosity of the high-chromium alloy electrode with small holes whose diameter were less than 1 μm resulted in mono-periodic current oscillations with small amplitude. Then, larger holes with diameters of over 3 μm gradually formed during the polarization process. The larger holes increased the peak current value of current oscillations, and finally contributed to the occurrence of the mix-mode current oscillations.

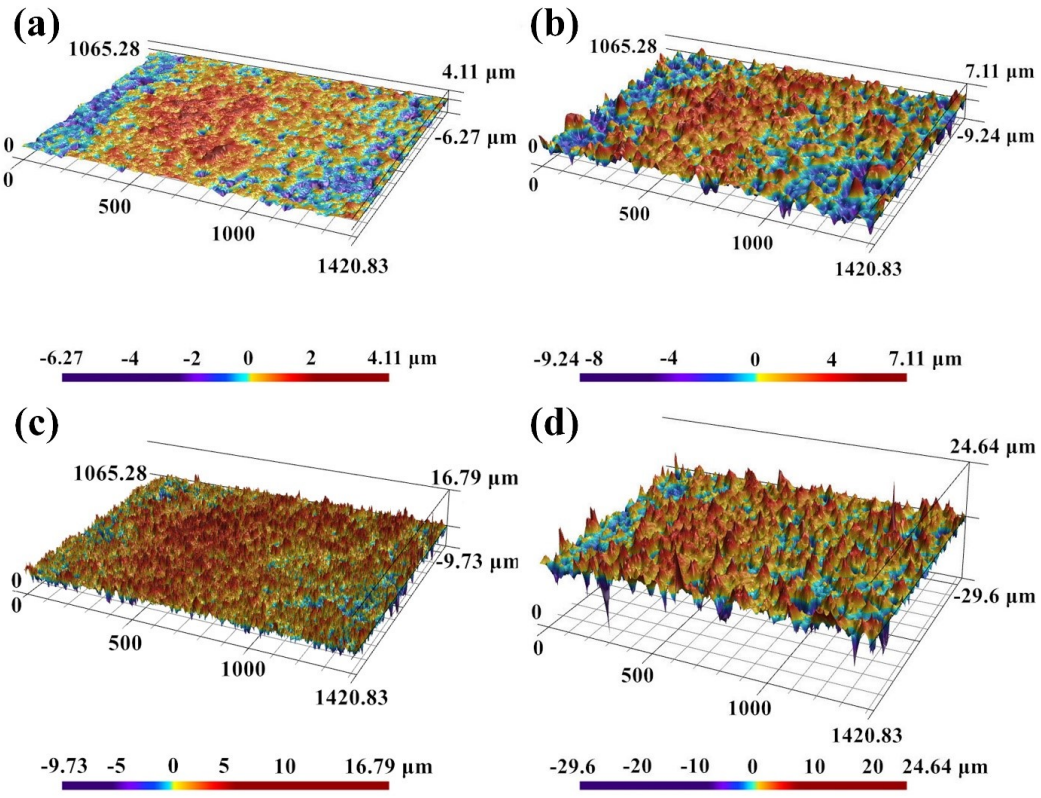

Fig. S1. LSCM images of the high-chromium alloy surface polarized potentiostatically under 6 $V_{Ag/AgCl}$ for different time: (a) 20 s, (b) 40 s, (c) 80 s, and (d) 120 s.

Thickness of the dealloyed layer and corrosion depth

Thickness of the electrochemical dealloyed layer and surface corrosion depth under different dealloying time were investigated. The cross section was magnified by angle section-view to accurately measure the thickness. Pretreated workpieces were mounted on special fixtures to form an angle of approximately 5.74°. The entire part was sealed with epoxy resin to protect the surface from damage in the subsequent polishing process. The angle section-view digital image was shown in Fig. S2 (a), and measurement results were displayed in Fig. S2 (b). Thickness of the dealloyed layer could be adjusted by changing the dealloying time, and the thickness was ~9.7 μm after 60 s. Surface profile tests were carried out to measure depth of surface corrosion, and the profile (pretreated under 6 V vs. Ag/AgCl for 100 s) was shown in Fig. S2 (c). The profile contained two parts: unaffected zone, and dealloyed zone. The corrosion depth was the difference value between average profile height of the unaffected zone and average peak height of the dealloyed zone. Measurement was repeated 3 times on each workpiece, and variation of dissolution depth with time was shown in Fig. S2 (d). Anodic surface was rapidly corroded in the beginning; after 60 s, the corrosion rate decreased. The corrosion depth linearly increased with time until reached 1.74 μm at 100 s.

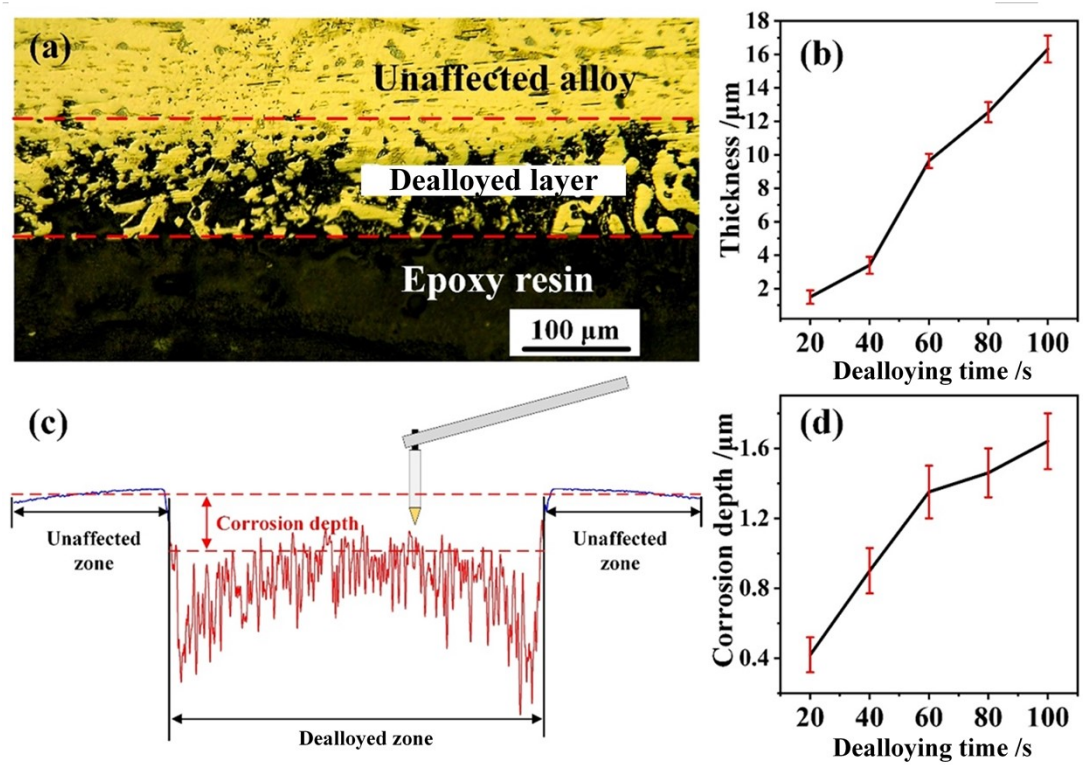

Fig. S2. Thickness of the dealloyed layer and corrosion depth. (a) Angle section-view digital image of the dealloyed layer, (b) thickness of dealloyed layer vs. dealloying time, (c) surface profile of sample electrochemical dealloyed under 6 V vs. Ag/AgCl for 100 s and (d) corrosion depth vs. dealloying time.

Single grain scratching experiments

Single grain scratching experiments were performed on to further investigate the effect of the dealloying process on deformation resistance and machinability of the alloy. Scratching experiments with linearly increasing scratching depth were performed on untreated and dealloyed ultra-high chromium surfaces (electrochemical dealloyed for 60 s). The surfaces were mounted on an angular shift stage installed on a computer numerically controlled precision platform. Angles could be adjusted from plus 20° to minus 20° in both X-Z and Y-Z planes. The variation of scratching depth could be controlled by adjusting the deflection angle of the angular shift platform, a 3-axis piezoelectric dynamometer (Kistler, 9526C1) was settled under the platform to measure forces during the single grain scratching processes, as shown in Fig. S3. During the scratching experiments, the scratching depth increased by 1 μm under the scratching length of 0.3 mm. The feed rate was set as 0.5 mm/s, and the scratching length was 10 mm. Before scratching, the indenter slowly approached the ultra-high chromium surfaces. When the indenter contacted with the workpiece, the force sensor would detect a sudden change, and the indenter position at this moment was regarded as the zero point of the test co-ordinate.

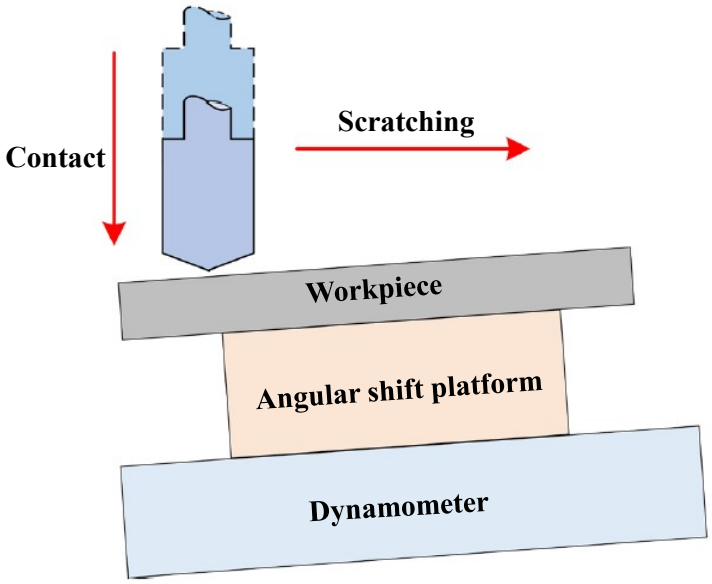

Fig. S3. Schematic diagram of the scratching process with linearly increasing depth

Shown in Fig. S4 were the scratch morphologies of untreated and electrochemical pretreated ultra-high chromium steel surfaces with linearly increasing scratching depth. For the untreated surface, there were a large number of bulges caused by plastic flow. In addition, scale-like deformation structures could be observed at the bottom of the scratch. With increasing of the scratching depth, the bulges and scale-like structures became more obvious. By contrast, no significant bulges were found on each side of the scratches on the electrochemical pretreated surface, and only a small amount of scale-like deformation structures were observed at the bottom of the scratches with larger scratching depths. This was because the loose porous structures formed by the electrochemical pretreatment collapsed in the indentation direction under the extrusion of the diamond grains. Therefore, the materials would not flow plastically to each side of the scratch.

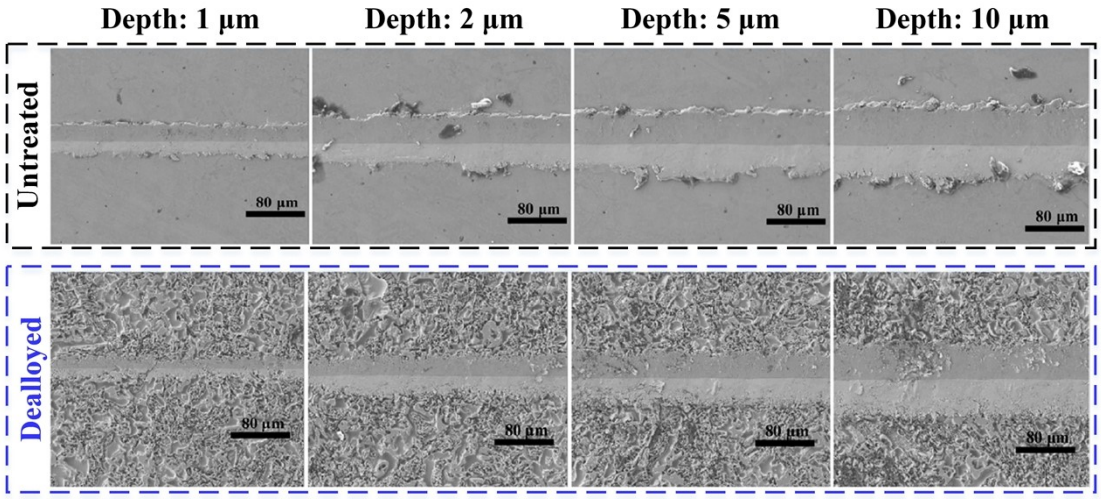

Fig. S4. Scratch morphologies of untreated and electrochemical dealloyed ultra-high chromium steel surfaces with linearly increasing scratching depth

As shown in Fig. S5, compared with the untreated surface, the scratching forces of electrochemical dealloyed surface were significant lower. When the scratching depth was 2 μm, the normal and tangential scratching forces of the untreated surface were about 0.486 N and 0.304 N, while those of the dealloyed surface were just ~0.051 N and 0.037N, decreased by about 90%. When the scratching depth was larger than the electrochemical pretreatment layer (~10 μm), the reduction ratio decreased gradually.

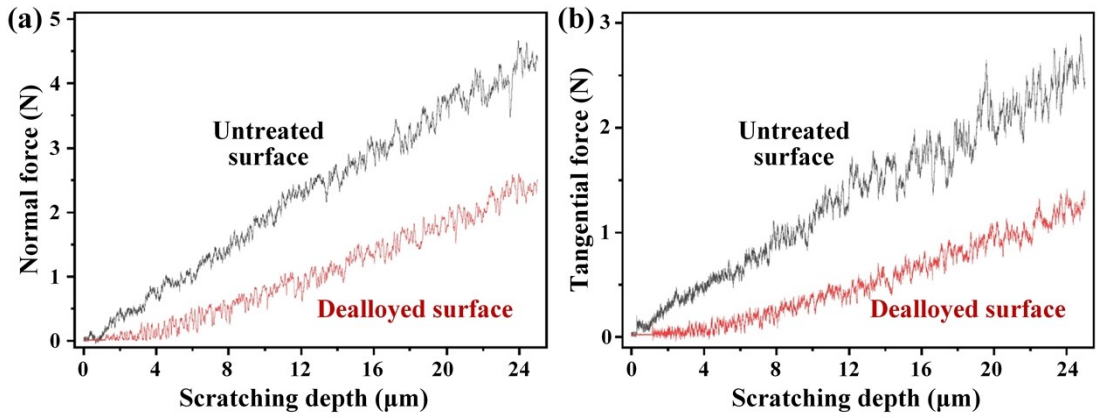

Fig. S5. Scratching forces of untreated and electrochemical pretreated surfaces: (a) normal force, (b) tangential force

Therefore, appropriate cutting depth could be determined during the machining process according to the depth of the porous structures. When the cutting depth is slightly larger than the depth of the porous structures, machinability of the alloy can be well improved (because the main removal part has much lower strength); in addition, the porous structures can be removed, thus not influencing further application of the alloy.